Defence Science Journal, Vol. 58, No. 2, March 2008, pp. 200-208

Inelastic Deformation Behaviour of Polypropylene in Large Strain Region and after Cyclic Preloadings

Kenji Kaneko

Tokyo University of Science, 1-3 Kagurazaka, Tokyo, 162-8601

ABSTRACT

Inelastic deformation behaviour of polypropylene in tensile large strain region and after axial pre-cyclings is investigated experimentally and analysed using the three-element model based on the overstress theory. In this experiment, cylindrical tubular specimen as well as solid bar specimen are used for torsional loading and volume change is measured to get the true stress-true strain curves. It is found that flow stress is almost constant in strain range of more than 0.1, Poisson's ratio varies depending on strains and the viscosity does not change even after cyclic preloadings in tension, torsion, and compression. The quasi-static stress-strain curve g is represented as a function of temperature. Good agreement can be obtained between predicted results based on obtained constitutive equations having the first invariant of stress (static pressure) effect and the experimental results on both the flow stress and relaxation.

Keywords: Constitutive equations, overstress theory, inelasticity, large strain, polypropylene, visco-plasticity, tension, torsion, compression, cyclic preloading, hydrostatic pressure, relaxation

1. INTRODUCTION

Polypropylene (PP) is one of the familiar polymers usually used as a functional material in many fields in electronics and medicine, but its use is restricted in the area where material strength is not much needed, because PP is inferior to metals in stiffness, strength, and temperature properties, and its deformation properties are difficult to estimate. So, if its deformation properties become easier to estimate for various conditions of temperature and loading, the PP, which is lighter and cheaper than metals and incapable of recycle, can be used extensively as parts of machine and in construction.

Many studies[1-8] were reported on deformation properties of PP in simple loading as tension, compression, and torsion, but in most of the reports, nominal stress-strain curves were obtained and Poisson ratio was assumed to be 0.5.

Generally, polymers are compressible materials, but in many studies, stress is estimated on the assumption of incompressibility in testing tensile properties. So, a considerable error may be involved in the constitutive equations. In this study, the volume change of the specimen has been measured in the tests.

Loading direction dependency of deformation properties is investigated by torsional data as well as axial loading test data. As many studies[2,4,9-14] on cyclic loading properties have been reported, the effect of cyclic preloading on subsequent tensile properties is investigated. On the basis of the overstress model, result obtained are rearranged and the constitutive equations with effects of temperature, strain rate, and the first invariant of stress are formed.

Received 31 October 2007

2. EXPERIMENTAL

2.1 Experimental Apparatus

The electro-hydraulic servo-controlled fatigue testing machine by Shimadzu EB50kN and the computer-controlled axial-torsional combined stress testing system were used for the tests.

Temperature of the specimen is PID-controlled in the thermostatic chamber with heated air nozzles. Each test starts 30 min after the temperature becomes stable.

2.2 Specimens

Specimens for tensile test were machined from a round bar of 20 mm dia (made of E209-pellet supplied by Mitsui Chemical Corp). The parallel length of the specimen was 30 mm and the parallel dia was 12 mm. The specimens for the combined stress tests were machined from a round bar of 30 mm dia. The dimensions of the thin walled tubular specimen were 20 mm in outer dia and 2 mm in thickness at the parallel part.

Strains of specimen were measured using the extensometer and the diameter displacement meter for axial tests and the rotational displacement meter for torsional tests[12,15-16].

2.3 Experimental Conditions

2.3.1 Loading Conditions for the Tubular Specimens

Tension, compression, and torsion tests were performed at 290 K during the strain range of ± 3 per cent in definition of von Mises effective strain, at three kinds of strain rates of $\dot{\varepsilon}=1\times10^{-2}\,1/\mathrm{s},\ 1\times10^{-3}\,1/\mathrm{s},\ 1\times10^{-4}\,1/\mathrm{s}$. 2000 s stress relaxation test followed after prestraining to 3 per cent.

2.3.2 Loading Conditions for the Round Bar Specimens

Tensile tests with sudden changes in strain rate were performed after preloadings. This is because the viscosity of the material can be estimated by only one specimen with no error due to the variance in property among specimens. Loading conditions are as follows:

- Temperatures of the experiments: T = 303 K, 323 K, 343 K
- Number of cycles n = 0, 1, 5, 10-times
- Cyclic strain ranges $\Delta\varepsilon = \pm 0.05, \pm 0.07, \pm 0.09$
- Strain rate at cyclic loading: $\dot{\varepsilon}=1\times10^{-3}\,1/\mathrm{s}$
- Strain rates at reloading: $\dot{\varepsilon}=1\times10^{-3}1/\mathrm{s},10^{-4}\,1/\mathrm{s},\ 10^{-5}\,1/\mathrm{s}$
- Stress relaxation at the points of prestrain: ε_{pr} = 0.19, 0.27, 0.35.

3. EXPERIMENTAL ANALYSIS

3.1 Overstress Model

The three-element model consisting of one spring, one dash pot, and one slider, used in experimental analysis is shown in Fig. 1. Mechanical properties of each element were expressed as the functions of strain ε, strain rate $\dot{\varepsilon}$, and temperature T. So, most of the actual elastic visco-plastic deformation behaviours can be expressed precisely with such a simple model. The flow stress g of the slider element in the model is called quasi-static (or equilibrium) stress, which appears at strain rate $\dot{\varepsilon}=0$ or after a long time relaxation.

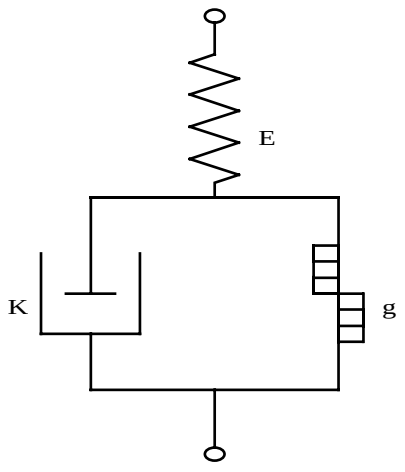

Figure 1. Elastic-visco plastic constitutive model.

3.2 Constitutive Expressions for Simple Loading, Creep, and Relaxation

The general expression between a total strain rate and a flow stress is

$$\dot{\varepsilon} = \dot{\varepsilon}^e + \dot{\varepsilon}^p = \frac{\dot{\sigma}}{E} + \frac{\sigma - g}{K E} \quad (1)$$

where ε^e is the elastic strain ε^p is the plastic strain, E is the elastic modulus, σ is the flow stress, g is the quasi-static stress, and K is the viscosity function.

4. EXPERIMENTAL RESULTS

4.1 Hydrostatic Pressure Dependency of Flow Stress

Figure 2 shows the stress-strain curves for tensile/compressive and torsional loadings at room temperature (290 K) using tubular specimens. The effective stress-strain relation of von Mises type is used for analysing torsional test results.

Equivalent elastic shear modulus is $3G$ and is not equal to Young's modulus E. So, an elastic strain is eliminated from total strain. Loading direction dependency, which means the effect of the first invariant stress: $I_1 = \sigma_1 + \sigma_2 + \sigma_3$, of flow stress can be seen clearly, as shown in Fig. 2, where σ_{1-3} means the principal stresses.

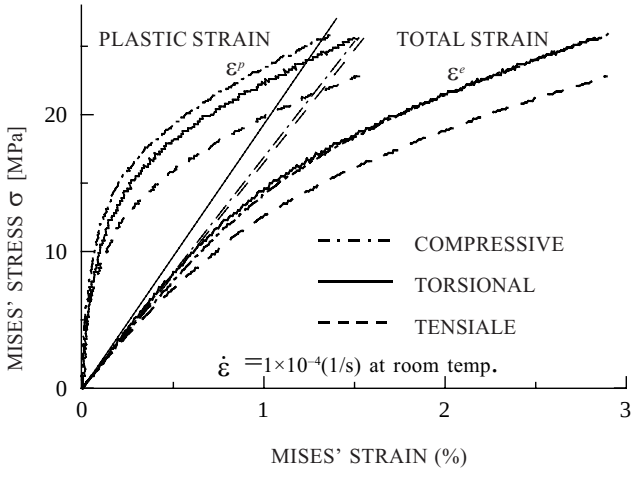

Figure 2. Stress-strain curves for different loading directions.

Figure 3 shows the effect of the first invariant of stress on flow stress differences $\Delta\sigma$ $(=|\sigma_{ten}+\sigma_{comp}|/2)$ between tensile and compressive stress-strain curves obtained at three different temperatures and at strain rate $\dot{\varepsilon} = 10^{-4}\,1/\mathrm{s}$. The stress differences are represented by the following equation:

$$\Delta\sigma = kI_1 \quad (2)$$

The coefficient k is decided –0.06 (constant) as to be simple by making reference to data[13,17].

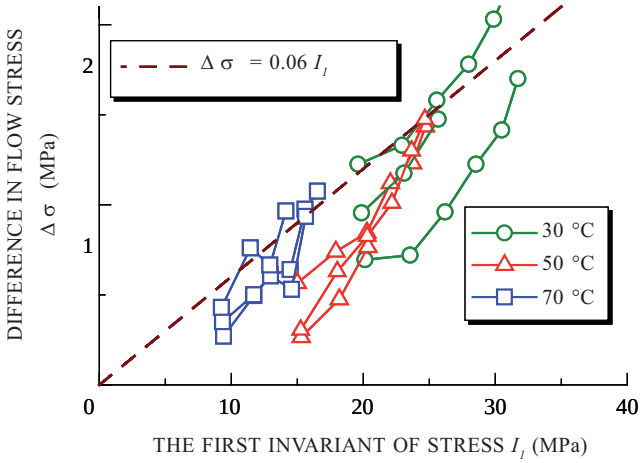

Figure 3. Effect of temperature on hydrostatic pressure dependency of flow stress.

4.2 Poisson Ratio and True Stress-strain Curves in Tensile and Compressive Loadings

Figure 4 shows the strain dependence of Poisson ratio in tensile and compressive loadings.

A constant volume expansion was observed in tension, but a temporal contraction in compression was observed initially, incompressibility appeared at a large strain range in compression.

Figure 5 shows the comparisons between stress-strain curves, one of which is calculated on the assumption of incompressibility and the other on the way of using true Poisson ratio. A large error appeared at strain range of > 5 per cent.

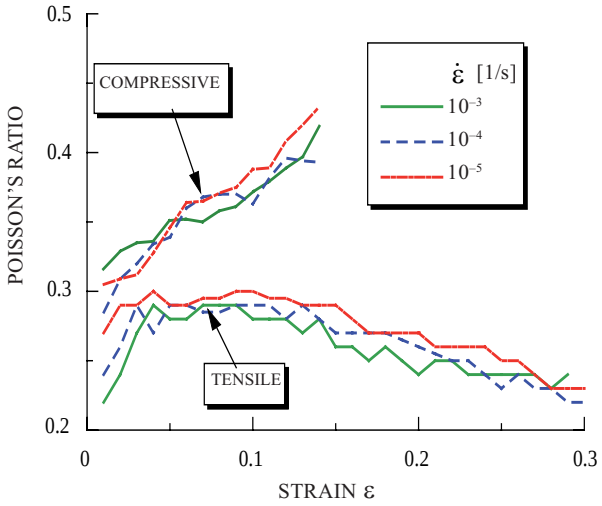

Figure 4. Real Poisson's ratio depending on the hydrostatic pressure.

4.3 Temperature and Prestrain Dependency of Flow Stress and Viscosity

Figure 6 shows tensile true stress-strain curves after cyclic loading at three different temperatures, where strain rate was changed suddenly several times to estimate viscosity. Cyclic loading conditions appear in the figure. Considerable reductions in both the stress and viscosity could be observed with increase in temperature, but almost no change in stress and viscosity occured with increase in strain at range of > 10 per cent.

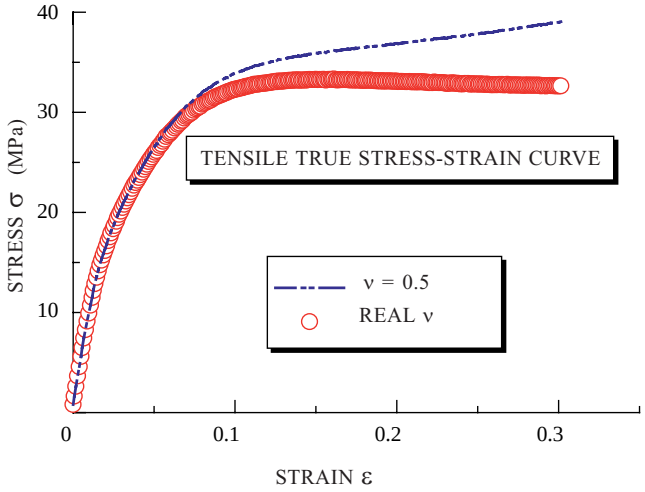

Figure 5. Real stress-strain curve obtained using real Poisson's ratio comparing with the curve based on incompressibility hypothesis.

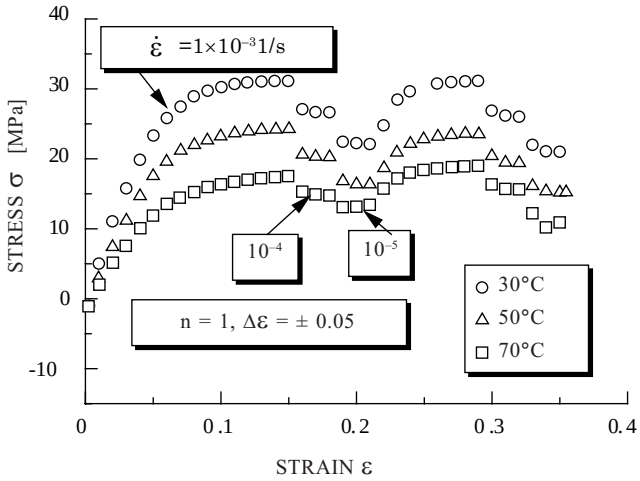

Figure 6. Stress-strain curves after cyclic prestraining.

4.4 Cyclic Preloading Dependency of Flow Stress and Viscosity

Figures 7 and 8 show tensile stress-strain curves after various cyclic preloadings at elevated temperatures where strain rate was changed suddenly several times.

Decrease in flow stress was observed with an increase in number of cycles in a cyclic hysteresis loop[9-11, 13-14]. In the figures, stress in reloading was found to keep the cyclic softening, but the stress decrease was negligibly small in comparion to the variance of specimens and temperature dependency of the stress.

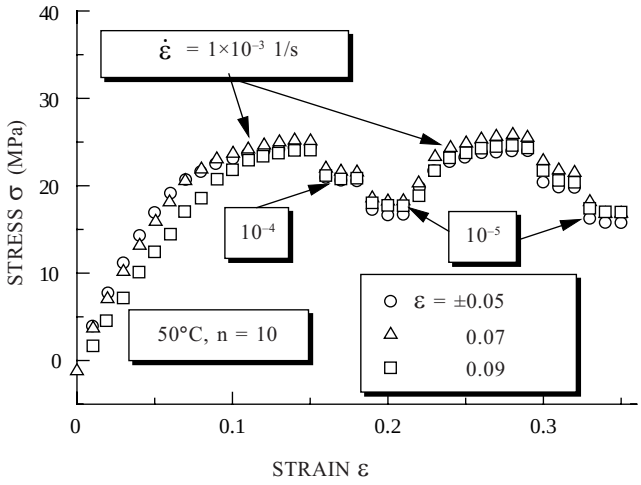

Figure 7. Stress-strain curves after cyclic prestraining.

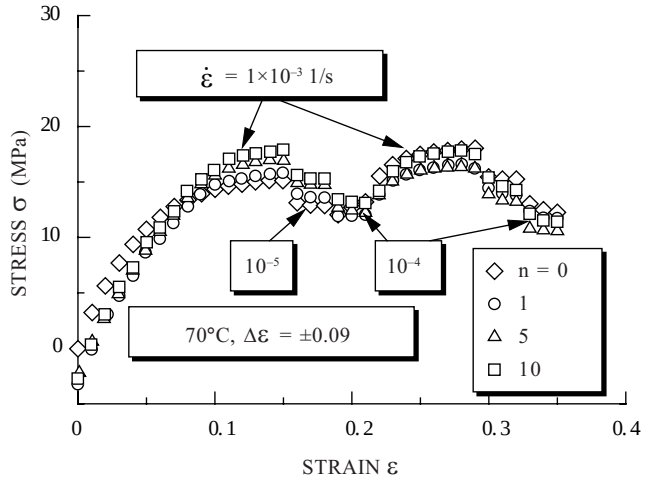

Figure 8. Stress-strain curves after cyclic prestraining.

Figure 9 shows stress relaxation curves after prestraining at ε = 0.15 or 0.30 at strain rate of $\dot{\varepsilon} = 1\times10^{-3}\,1/\mathrm{s}$ at 30 °C, and other curve after cyclic preloading of $\Delta\varepsilon = \pm 0.09,\ n = 10$ and after prestraining up to ε = 0.35 were involved. Almost no difference could be observed among these. So, it is confirmed that viscosity is independent of cyclic loading in a large strain range in reloading.

5. MATERIAL CONSTANTS BASED ON OVERSTRESS CONSTITUTIVE MODEL

It has been confirmed that constitutive relations based on the overstress model give good predictions on simple tensile, compressive, and torsional loading properties for many kinds of polymers[1,2,4,6,8].

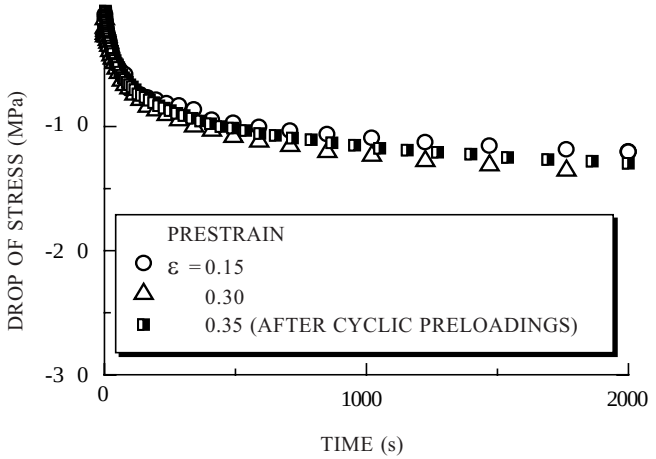

Figure 9. Comparisons between relaxation curves obtained after simple tensile prestraining and cyclic prestraining.

In this report, material constants have been presented for polypropylene for the wide strain range from – 0.15 to 0.35 as the functions of temperature.

5.1 Initial Elastic Coefficients

Initial elastic coefficients were slightly depending on strain rate, but were constant at strain range of < 0.0005 (0.05 %) in both tension and compression. In this paper, the initial elastic coefficient is presented as the function of temperature as

$$E = -16.1T\left[\mathrm{K}\right] + 5950 \ \ [\mathrm{MPa}] \tag{3}$$

5.2 Quasi-static Stress-strain Curve

In the overstress constitutive model, the quasi-static stress *g*, which is corresponding to strain rate $\dot{\varepsilon} \approx 0$, was used as the base stress. The stress *g* can not be obtained directly through experiment, so it was determined by the extrapolation method as shown in Fig. 10, where the flow stresses are calculated as the average of tensile and compressive stresses so as to eliminate the hydrostatic pressure dependence.

In this paper, the stress *g* is corresponding to the strain rate of $\dot{\varepsilon} = 10^{-11}\,1/\mathrm{s}$. Solid lines are made on the approximated expression: $\log_{10}\sigma = a + b(\log_{10}\dot{\varepsilon} + 11)^n$ in Fig. 10. So, the stress is also expressed as $\sigma \equiv g = 10^a$. The quasi-static stress-strain curve $g(\varepsilon, T)$ is represented by Eqn (4) as a function of temperature. Figure 11 shows the calculated $g(\varepsilon, T)$ curves using Eqn (4) as

$$g\left(\varepsilon, T\right) = (p\,\varepsilon + q)\tanh(r\varepsilon) \tag{4}$$

where $p = 21.2 - 0.05T$, $q = 80.0 - 0.218T$, $r = 32$.

5.3 Formulation of the Viscosity Function *K*

The overstress (viscous stress) $X = \sigma - g$ can be determined after $g(\varepsilon, T)$ stress is decided.

In this paper, *K*-value is calculated using a total strain rate even at the elastic-plastic strain range of < 0.1. Thus obtained *K*-value is not constant but is a function of strain as well as overstress and temperature. Figure 12 shows *K*-value plotted to

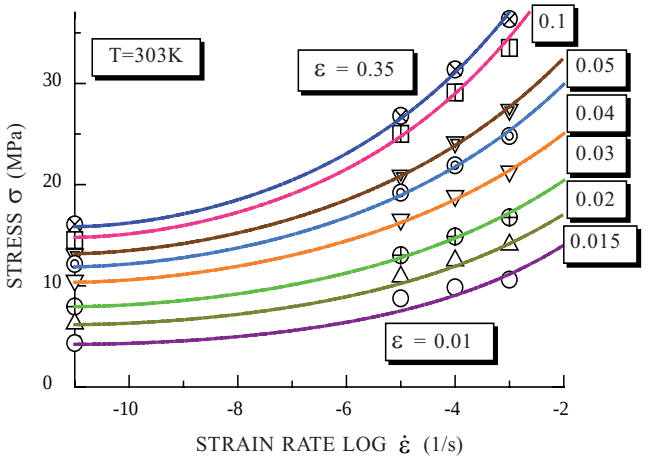

Figure 10. Determination of quasi-static stresses.

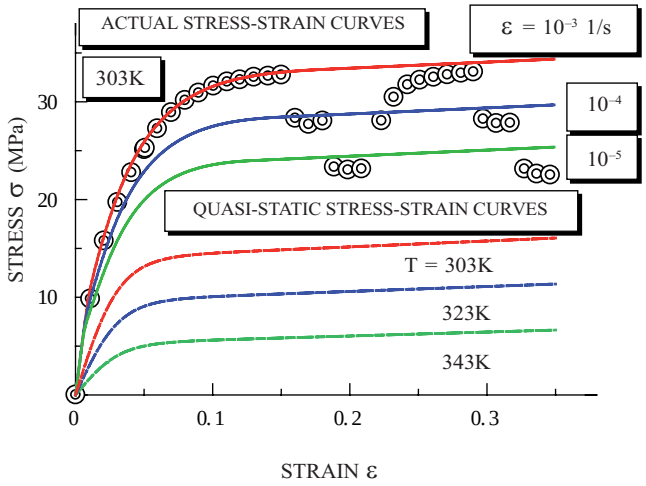

Figure 11. Quasi-static stress-strain curves for three kinds of temperature

the overstress X with a parameter of strain ε. As shown in Fig. 12, $\log_{10} K$ is linear to the overstress X for polypropylene and is expressed in Eqn (5), where K_1 means a gradient and K_2 a section value cut by X-axis coordinate of the approximated line shown in Fig. 12.

$$\log_{10} K = -K_1 (X - K_2) \quad , \tag{5}$$

where

$$K_1 = (A_1\ \varepsilon\ +\ B_1)\,\varepsilon^{-C_1},$$

$$A_1 = 0.003898T - 1.039,$$

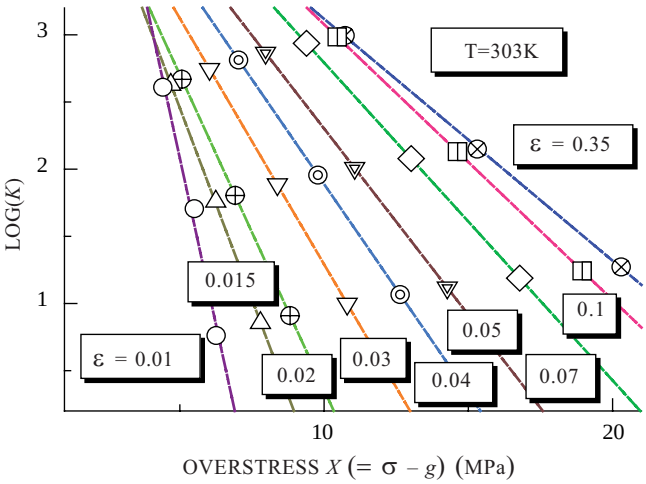

Figure 12. Relationship between the viscous coefficient and the overstress at 30 °C depending on strain.

$$B_1 = -0.0004180T + 0.1545,$$

$$C_1 = 0.00745T - 1.572,$$

$$K_2 = A_2\ \tanh(B_2\ \varepsilon)\ +\ C_2,$$

$$A_2 = -0.1768T + 76,$$

$$B_2 = 0.003863T^2 - 2.426T + 397.4,$$

$$C_2 = -0.0642T + 24.0.$$

6. COMPARISON BETWEEN PREDICTED AND EXPERIMENTAL RESULTS

6.1 Calculation Methods

When stress-strain curves are required for a given strain rate, flow stress is calculated using the following equation derived from Eqn (1):

$$\sigma = g + \left(E - \frac{d\sigma}{d\varepsilon} \right) \dot{\varepsilon} \cdot K \tag{6}$$

A given strain rate $\dot{\varepsilon}$ an elastic modulus E by Eqn (3), a present strain ε, a strain increment $d\varepsilon$ and a quasi-static stress g are substituted in the Eqn (6). Although K-value is expressed by Eqn (5), K-value can not be obtained directly, because $X = \sigma - g$ is unknown value. So, it is necessary to get a set value of K and X by an iterative calculation.

Thus, obtained stress-strain curve is corresponding to a torsional loading. The stress $\Delta\sigma$ of Eqn (2) due to hydrostatic pressure is added for compression but eliminated for tensile loading.

For predicting stress relaxation properties, the following equation derived from Eqn (1) is used:

$$d\sigma = -\frac{\sigma - g}{K} dt \tag{7}$$

6.2 Comparison between Predicted and Experimental Results

Figure 13 shows predicted tensile stress-strain curves at three different strain rates and at three different temperatures, compared to the corresponding experimental results, where strain rate is changed several times while loading to set the viscous stress eliminating the variance in property among specimens. In the figure, the solid line, the alternate long and short dash line, and the broken line mean the results for strain rate of $\dot{\varepsilon}$=10^{-3}1/s,10^{-4}1/s,10^{-5}1/s , respectively.

The predicted results not necessarily agree with the experimental results. The main reason for the disagreement is the variance in property among the specimens. Poisson ratio in tension sometimes takes larger values than that shown in Fig. 4. This fact is also one of reasons for the disagreement.

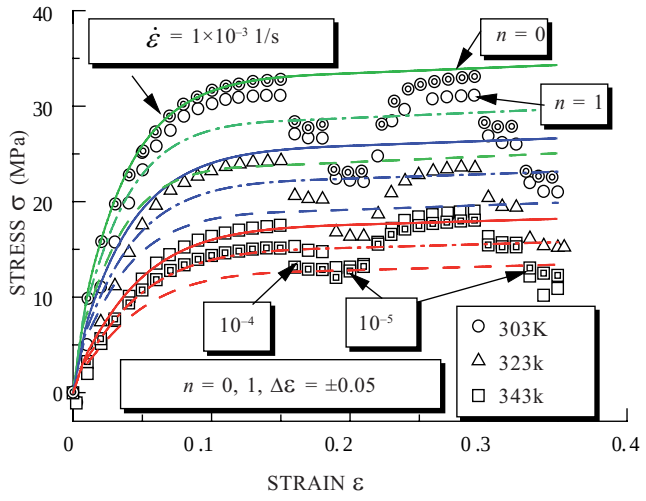

Figure 13. Comparisons between experimental and predicted results on stress-strain curves.

Figure 14 shows comparison between predicted and experimental results on relaxation curve after tensile prestrainings at three different temperatures, where set of values of strain rate $\dot{\varepsilon}$ and prestrain ε_{pr} are as follows:

$$\left(\dot{\varepsilon}, \varepsilon_{pr}\right) = (10^{-5}, 0.19), (10^{-4}, 0.27), (10^{-3}, 0.35)$$

In the figure, the solid line, the broken line, and the alternate long and short dash line mean the predicted results after loading at strain rates of $\dot{\varepsilon}$=10^{-3}1/s,10^{-4}1/s,10^{-5}1/s , respectively. Although the presented expressions cover broader fields, good agreements can be seen on the whole.

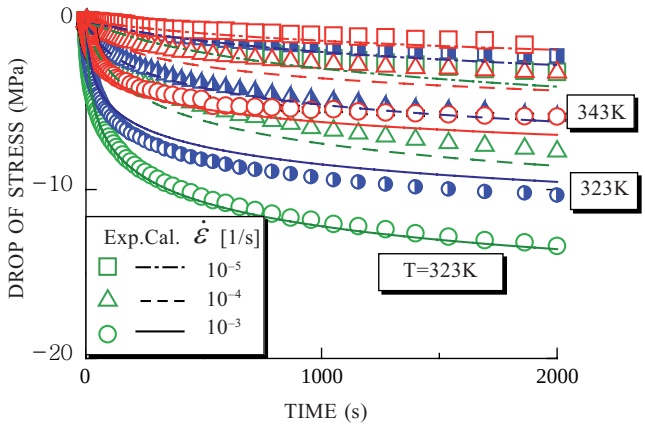

Figure 14. Comparisons between experimental and predicted results on relaxation curves for various strain rates and various temperatures.

Figure 15 shows the tensile and compressive stress-strain curves compared with the predicted ones at three different temperatures. Although some differences are observed due to variance in property among the specimens, the effect of the hydrostatic pressure on flow stress is clearly considered in the predictions. Figure 16 shows the stress relaxation curves at prestrain of 0.03 by tension, torsion, and compression. Viscosity may appear depending on loading direction, but the differences among these relaxation curves are due to the hydrostatic pressure effect. That is, although the quasi-static stress and the viscosity is independent of loading direction, the overstresses differ from each other at the beginning of each relaxation test because the flow stress depends on the loading direction. The results shown in

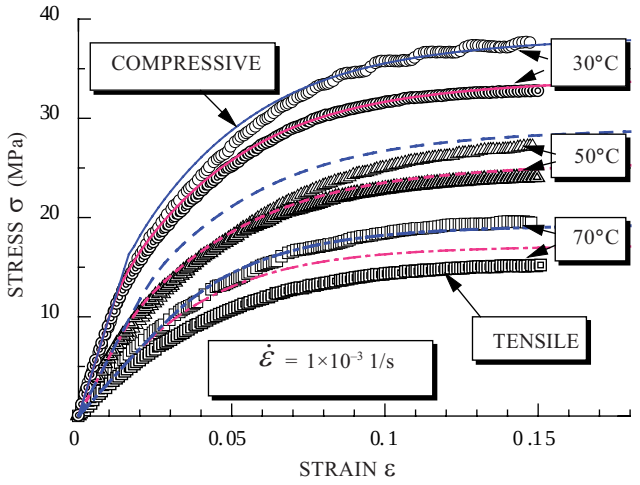

Figure 15. Comparisons between experimental and predicted results on tensile/compressive stress-strain curves for various temperatures.

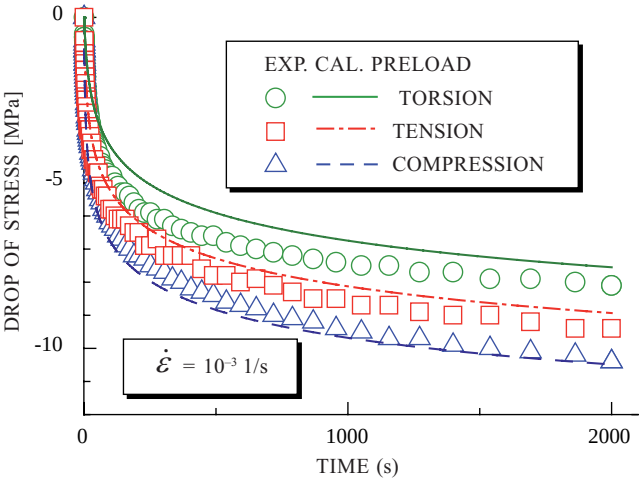

Figure 16. Comparisons between experimental and predicted results on relaxation curves obtained after tensile, torsional and compressive preloadings, respectively.

Fig. 16 also confirm the analytical methods and the constitutive expressions presented in this paper. The experimental results of Fig. 16 were obtained at 290 K.

7. CONCLUSIONS

In this paper, the true stress-strain curves including cyclic hysteresis loops, of tension, torsion, and compression at various temperatures and at various strain rates are obtained experimentally.

Analysing these experimental data, it is confirmed experimentally and analytically that viscosity and quasi-static stress are independent of loading direction and viscosity is not affected by cyclic loading.

Considering the effects of the hydrostatic pressure and temperature on a true flow stress, the constitutive relations were presented and confirmed to express the elasto-visco plastic deformation behaviours of broad strain range precisely and systematically.

ACKNOWLEDGEMENTS

The author would like to express great appreciation for the members of the workshop by Tokyo University of Science for their support and cooperation, and also thank the fellow graduate students and undergraduate students, Dr Takanobu Oyamada (1994, DC), Mr Naoki Sakai (1996, UG), Mr Ichirou Suzuki and Mr Osayuki Yoshida (1997, UG) and Mr Takashi Nishiyama (2001, MC) for their help.

REFERENCES

1. Ariyama, T.; Mori, Y. & Kaneko, K. Effects of strain rate and temperature on the deformation behaviour of polypropylene. *Trans. Japan Soc. Mech. Engrs.*, 1996, **62**(595), 781-86.

2. Ariyama, T.; Mori, Y. & Kaneko, K. Tensile properties and stress relaxation of polypropylene at elevated temperatures. *Polymer Engg. Sci.*, 1997, **37**, 81-90.

3. Bordonaro, C.M. & Krempl, E. The effect of strain rate on the deformation and relaxation behaviour of 6/6 nylon at room temperature. *Polymer Engg. Sci.*, 1992, **32**(16), 1066-072.

4. Hiroe, T.; Matsuo, H.; Fujiwara, K. & Tsuda, Y. Time-temperature equivalence for the stress-strain behaviour of high density solid polymers. *Trans. Japan. Soc. Mech. Engrs.*, 1998, **64**(624), 2087-092.

5. Kitagawa, M.; Mori, T. & Matsuya, T. Stress-strain curve of polypropylene. *Trans. Japan. Soc. Mech. Engrs.*, 1989, **55**(512), 923-28.

6. Kitagwa, M.; Zhou, D. & Qiu, J. Stress-strain curves for solid polymers. *Polymer Engg. Sci.*, 1995, **35**(22), 1725-733.

7. Krempl, E.; McMahon, J.J. & Yao, D. Viscoplasticity based on overstress with a differential growth law for the equilibrium stress. *Mechanics of Materials*, 1986, **5**, 35-48.

8. Krempl, E. & Bordonaro, C.M. A state variable model for high-strength polymers. *Polymer Engg. Sci.*, 1995, **35**(4), 310-16.

9. Ariyama, T.; Sakuma, T. & Kaneko, K. Visco-elasto-plastic behaviours of polypropylene after cyclic preloadings. *Trans. Japan. Soc. Mech. Engrs.*, 1992, **58**(556), 2345-350.

10. Ariyama, T. Cyclic deformation and relaxation characteristics in polypropylene. *Polymer Engg. Sci.*, 1993, **33**(1), 18-25.

11. Ariyama, T. Stress relaxation behaviour after cyclic preloading in polypropylene. *Polymer Engg. Sci.*, 1993, **33**(22), 1494-501.

12. Kaneko, K. Plastic constitutive model of the initial anisotropic metals after superposed prestrainings. *Trans. Japan. Soc. Mech. Engrs.*, 1994, **60**(580), 2759-766.

13. Kitagawa, M. & Qiu, J. Effect of strain history and pressure on cyclic torsional stress-strain curves for crystalline polymers. *Trans. Japan. Soc. Mater.,* 1992, **41**(461), 225-30.

14. Kitagawa, M.; Qiu, J.; Nishida, K. & Yoneyama, T. Cyclic stress-strain curves at finite strains under high pressures in crystalline polymers. *J. Mater. Sci.*, 1992, **27**, 1449-457.

15. Ariyama, T. & Kaneko, K. A constitutive theory for polypropylene in cyclic deformation behaviour. *Polymer Engg. Sci.*, 1995, **35**, 1461-467.

16. Kaneko, K. A plastic constitutive model for anisotropic hardening metals. *Euro. J. Mech. A/Solids*, 1995, **14**(5), 679-96.

17. Mears, D.R.; Pae, K.D. & Sauer, J.A. Effects of hydrostatic pressure on the mechanical behaviour of polyethylene and polypropylene. *J. Appl. Phy.,* 1969, **40**(11), 4229-237.